Joint Source-Channel Coding with Unequal Error Protection using Asymmetric Turbo Codes

Hanxin WANG, Cuitao ZHU, Chengyi XIONG and Shaoping CHEN

Department of Electronics and Information Engineering, South-Central University for Nationalities, Wuhan, China

wanghx8888@163.com, zhucuitao@163.com, xiongchengyi@qq.com, spchen@scuec.edu.cn

***Abstract*—In this paper, we devise an efficient joint source-channel coding scheme for robust image transmission over noisy channels. We firstly present a novel interleaver, named unequal row column cyclic cross interleaver, which could improve the error correction capability of turbo codes effectively. Secondly, we devise two types of asymmetric turbo codes which consist of the parallel concatenated turbo codes using two non-identical component encoders with the different constraint lengths and mixed types of generator polynomials. The presented asymmetric turbo codes can optimize the bit error rate of both water-fall region at low signal to noise ratio and error-floor region at high signal to noise ratio, they outperform the conventional symmetric turbo codes but with reduced decoding complexity. Finally, we propose a joint source-channel coding scheme based on unequal error protection using asymmetric turbo codes. This scheme can adaptively adopt different coding strategies, different interleavers of turbo codes, various decoding algorithms and appropriate decoding iterative numbers according to the different significant levels of image data streams and the varying conditions of estimated channel state information. The proposed scheme can also dynamically adjust the source compression ratios and channel code rates by optimizing the rate allocation according to the calculated peak signal to noise ratio of reconstructed images and the estimated channel states information. The experimental results show that the proposed joint source-channel coding scheme can evidently increase the peak signal to noise ratio of the reconstructed images and improve the visual effect of the images but with no additional bandwidth, the scheme is more adaptive and feasible.**

***Index Terms*—Joint source-channel coding; Unequal error protection; Asymmetric turbo codes; Interleaver; Bit error rate; Water-fall, Error-floor; Peak signal to noise ratio**

I. INTRODUCTION

With the development of wireless multimedia communication services, the fast growing consumer demand has spurred more interest in the image and video data transmission over noisy channels. The varying wireless channel causes high transmission errors for multimedia data streams and results in deterioration of reconstructed image and video qualities. To enhance the efficiency and reliability of data streams, source data compression and channel errors correction technologies are two effective solutions in the digital multimedia communication. On the one hand, the source data have numerous redundant information which require to be processed. Compressed data streams are very sensitive to channel errors because their most redundancy bits are removed. Sometimes a few errors may destroy the entire data streams and thus affect the qualities of restored image and video. On the other hand, a large amount of channel errors could occur due to the poor wireless channels whose capacities are limited and time-varying. Considering the characteristics of both source data streams and channel state information (CSI), joint source-channel coding (JSCC) is a promising approach to achieve better performance in limited bandwidth and limited power system. JSCC technique has been attractive in delay-sensitive multimedia transmission system, especially in heterogenous networks where users may have different quality of service (QoS) requirements [1] [2]. JSCC has two main design issues. One is to design an appropriate channel protection method, and the other is to optimally allocate the given bandwidth resource between the source code and the channel code so as to achieve the best possible end-to-end performance in the noisy environment [3]. Unequal error protection (UEP) is an intelligent solution for JSCC. UEP is often applied to Forward Error Correction (FEC), the data bits are grouped according to some criteria capable of determining their importance to the restored source data, and the different channel codes are assigned to different source bit groups [4] [5] [6]. In recognition of the fact that the effects of bit errors in encoded sources are usually more detrimental in some bit groups than in others, several UEP schemes for image transmission using turbo codes are reported according to the significant levels of the image bit streams and varying channel characteristic [7], [8], [9]. But most of them mainly focus on UEP with conventional symmetric turbo codes (STC). However, STC evidently exist some defects that

Manuscript received May 3, 2012. This work was sponsored by the National Natural Science Foundation of China with Grant No.60972081, No.61072075, the Natural Science Foundation of State Ethnic Affairs Commission with Grant No.10ZN07 and the Key Project for the Natural Science Foundation of Hubei Province with Grant No.2009CDA139, it was also supported by International Fellowship Researcher of Chonbuk National University of Korea with Grant No. IFR2002.

Hanxin WANG is with the Department of Electronics and Information Engineering, South-Central University for Nationalities, Wuhan, China (Tel: 86-13343589736; fax: 86-027-67842815; email: wanghx8888@163.com)

Cuitao ZHU is with the Department of Electronics and Information Engineering, South-Central University for Nationalities, Wuhan, China (email: zhucuitao@163.com)

Chengyi XIONG is with the Department of Electronics and Information Engineering, South-Central University for Nationalities, Wuhan, China (email: xiongchengyi@qq.com)

Shaoping CHEN is with the Department of Electronics and Information Engineering, South-Central University for Nationalities, Wuhan, China (email: spchen@scuec.edu.cn)

they have either a good water-fall performance at low signal to noise ratio (SNR) or a good error-floor at high SNR, but not both over the entire range of SNR [10]. Asymmetric Turbo codes (ATC) are the better choice among the improvement of performance, the overall time delay and the computational complexity of decoding algorithms. Several ATC are investigated to improve bit error rate (BER) in the whole SNR ranges compared with STC [11], [12]. This paper presents an effective JSCC design based on UEP using ATC, which can adaptively adopt different coding strategies, different interleavers of turbo codes, various decoding algorithms and appropriate decoding iterative numbers in terms of the different significant levels of source bit streams and the varying conditions of estimated CSI. This scheme can dynamically adjust the source compression ratios (CR) and channel code rates according to the calculated peak signal to noise ratio (PSNR) of the reconstructed images and the estimated channel conditions. The proposed scheme can also evidently increase PSNR of the images and improve the visual effect of the images but with no additional bandwidth. The remainder of paper is organized as follows. In section II, we present a novel interleaver named unequal row column cyclic cross (URCCC) interleaver, it could improve the error correction capability of turbo codes effectively. In section III, we devise two types of ATC using the different constraint lengths and mixed types of generator polynomials to optimize the BER performance of both water-fall and error-floor for turbo codes. In Section IV, focusing on the characteristic that the image data streams compressed by set partitioning in hierarchical trees (SPIHT) algorithm have different sensitivity to channel bit errors, we propose an efficient JSCC scheme with UEP using the designed ATC. The simulation results for JSCC are shown in section V and the conclusions are drawn in the last section.

II. UNEQUAL ROW COLUMN CYCLIC CROSS INTERLEAVER

The interleaver is one of the essential components for turbo codes and plays an important role in determining the performance and decoding computational complexity, because the interleaver directly affects the distance properties of the turbo codes. An interleaver is used between the two constituent encoders of turbo codes to provide randomness and produce high weight codewords. The design aim of a good code-matched interleaver is to eliminate low weight codewords with significant contributions to the error performance and to reduce the number of other low weight codewords which could not be eliminated [13], [14], [15]. Considering the drawbacks of common block and random interleavers which can not eliminate the more information bits correlation or not permute the low weight codewords sequence effectively, we present a new unequal row column cyclic cross interleaver, i.e. URCCC. This new interleaver can more thoroughly eliminate the information bits correlation than block and random interleavers, it can also permute the low weight codewords sequence into high weight codewords ones.

A. Algorithm of URCCC interleaver

To improve the BER performance of turbo codes significantly, the good interleaver can be implemented to avoid low weight codewords and to provide sufficient randomness for the input sequences. Many interleavers have been done on design of turbo codes. The block and random interleavers are the most commonly used in turbo codes. But they can not preferably produce the fewest output codewords sequence with low weight. An optimal interleaver should be able to generate the largest minimum codewords weight with the lowest number of codewords of that weight. So, a novel interleaver, named URCCC, is firstly proposed to offer superior performance for ATC design. The proposed algorithm of URCCC is described as follows:

Step 1: Information bits data are written into $m \times n$ block interleaver matrix in row wise from left to right and top to bottom, as shown in Figure 1 (a). For convenience of description, we set $m = 8$ and $n = 8$, the data in Figure 1 represents bits sequence number of information data.

Step 2: Odd row bits data are rearranged as follow formula (1) and even row data are reordered as formula (2), respectively. C_i denotes interleaver table, i is column number, n is column length, mod denotes modular arithmetic, k and p are adjustable parameters, $k < n$, $p < n$, k and p are relatively prime to n, while $k \neq p$. The process result is shown in Figure 1 (b).

$$C_i = (k \times i)(\mathrm{mod}\, n) + 1, \qquad 0 < i \leq n \tag{1}$$

$$C_i = (p \times i)(\mathrm{mod}\, n) + 1, \qquad 0 < i \leq n \tag{2}$$

Step 3: Odd column bits data are rearranged as follow formula (3) and even column bits data are reordered as follow formula (4), respectively. C_j is also interleaver table, j is row number, m is row length, a and b are adjustable parameters, $a < m$, $b < m$, a and b are relatively prime to m, while $a \neq b$. The process result is shown in Figure 1 (c).

$$C_j = (a \times j)(\mathrm{mod}\, m) + 1, \qquad 0 < j \leq m \tag{3}$$

$$C_j = (b \times j)(\mathrm{mod}\, m) + 1, \qquad 0 < j \leq m \tag{4}$$

Step 4: The interleaved bits data are read out from interleaver matrix of Figure 1 (c) in column wise from top to bottom and left to right.

The good interleaver design would be capable of providing sufficient randomness. For some special information bit streams, such as low weight and symmetric bit data, the different interleavers can obtain complete different interleaved effectivenss. E.g. the input bits sequence 100000010... 010000001, the output bits data sequence after the block interleaver are all the same as the original input sequence, as shown in figure 2 (a), it can't reach the purpose of interleaver. But using URCCC interleaver, the input sequence is well permuted randomly, it can avoid the appearance of the fixed point, as shown in figure 2 (b). Here, the data in Figure 2 represents information bits.

1	2	3	4	5	6	7	8
9	10	11	12	13	14	15	16
17	18	19	20	21	22	23	24
25	26	27	28	29	30	31	32
33	34	35	36	37	38	39	40
41	42	43	44	45	46	47	48
49	50	51	52	53	54	55	56
57	58	59	60	61	62	63	64

Fig. 1 (a)

4	7	2	5	8	3	6	1
14	11	16	13	10	15	12	9
20	23	18	21	24	19	22	17
30	27	32	29	26	31	28	25
36	39	34	37	40	35	38	33
46	43	48	45	42	47	44	41
52	55	50	53	56	51	54	49
62	59	64	61	58	63	60	57

Fig. 1 (b)

30	43	32	45	26	47	28	41
52	23	50	21	56	19	54	17
14	59	16	61	10	63	12	57
36	39	34	37	40	35	38	33
62	11	64	13	58	15	60	9
20	55	18	53	24	51	22	49
46	27	48	29	42	31	44	25
4	7	2	5	8	3	6	1

Fig. 1 (c)

Fig. 1. Design for URCCC interleaver
(a) step 1 (b) step 2 (c) step 3

1	0	0	0	0	0	0	1
0	0	0	0	0	0	0	0
0	0	0	0	0	0	0	0
0	0	0	0	0	0	0	0
0	0	0	0	0	0	0	0
0	0	0	0	0	0	0	0
0	0	0	0	0	0	0	0
1	0	0	0	0	0	0	1

Fig. 2 (a)

0	0	0	0	0	0	0	0
0	0	0	0	0	0	0	0
0	0	0	0	0	0	0	1
0	0	0	0	0	0	0	0
0	0	1	0	0	0	0	0
0	0	0	0	0	0	0	0
0	0	0	0	0	0	0	0
0	0	0	0	1	0	0	1

Fig. 2 (b)

Fig. 2. Effectivenss of the different interleaver
(a) Block interleaver (b) URCCC interleaver

B. Simulation and Analysis of URCCC interleaver

The BER performance simulations of URCCC interleaver used in turbo codes is shown in Figure 3. For the ease of comparison, the simulation results of block and random interleavers are also drawn. In simulation experiments, information bits size is 378, generator polynomials of two component codes for turbo codes are 13 and 15 (in octal), one half code rate, 4 iteration number for log-MAP algorithm, BPSK modulation, AWGN channel. It is observed that URCCC interleaver outperform conventional block and random interleavers.

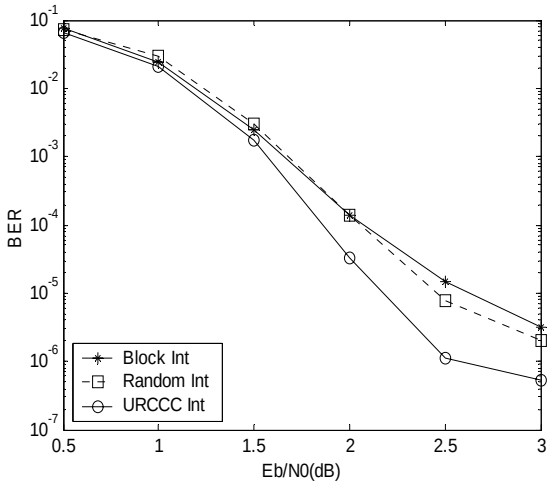

Fig. 3. BER versus E_b/N_0 for URCCC interleaver in turbo codes

URCCC interleaver can not only reduce the more information sequence correlation than block and random interleavers, it can also permute the low weight codewords sequence into high weight codewords sequence and significantly improve the performance of turbo codes. In the whole process of interleaving algorithm, URCCC interleaver are based on linear modular arithmetic, it has faster calculation speed and low complexity hardware requirement. For the process of row or column interleaving, it would complete only through the simple cyclic operation but not with a interleaving memory table, so it can save storage space. Moreover,

URCCC interleaver has adjustable parameters, it can dynamically select the parameters to adapt for various channel states and to improve the system error correction capability, the presented URCCC interleaver is more flexibility and robust.

III. ASYMMETRIC TURBO CODES

A. Review of Turbo Codes

Turbo codes have a near Shannon limit error correction capability through iterative decoding based on soft-input and soft-output (SISO) decoding algorithm. Turbo codes have been widely used in the wireless mobile communication system [16]. The conventional STC consist of two parallel concatenated recursive systematic convolutional (RSC) constituent encoders separated by an interleaver. Generally, these constituent encoders are the identical component codes with the same constraint lengths and the same generator polynomials [17], [18]. The BER performance curve of turbo codes is divided into two regions. The first region is called water-fall in lower SNR, the BER curve decreases rapidly at water-fall region. The second region is error-floor in higher SNR, the curve flattens in this region [10]. The STC have either good water-fall performance in lower SNR or good error-floor in higher SNR, but not both over the entire ranges of SNR. ATC are the better trade-off among the improvement of performance, overall delay and computational complexity of decoding algorithm. The performance evaluation of the ATC for the 3rd generation communication system (3G) are given in [11], [12].

ATC encoder is composed of two different parallel concatenated RSC1 and RSC2 encoder separated by an interleaver (Int), as shown in Figure 4. u_k is input information bit streams, x_k^s is the systematic information bits, x_k^{1p} and x_k^{2p} are the parity bits generated by RSC1 and RSC2, respectively. Puncturing of parity bits x_k^{1p} and x_k^{2p} can achieve the various required code rate. c_k is the coded bit streams which are consisted of x_k^s and x_k^p by parallel-to-serial (P/S) multiplexer.

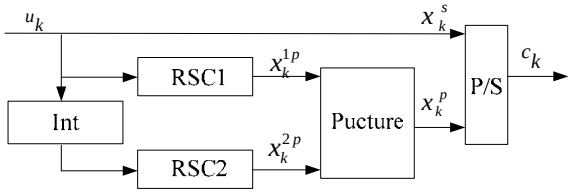

Fig. 4. ATC encoder

The coded bits c_k are then binary phase shift keying (BPSK) modulated and transmitted through an additive white Gaussian noise (AWGN) channel with a double sided power spectral density of $N_0/2$. At the receiver, the matched filter output y_k is multiplied by the channel reliability value L_c, as shown in Figure 5, $L_c = 4 \cdot (E_b / N_0) \cdot R$, where E_b / N_0 denotes received bit energy to noise power ratio and R represents the code rate [16]. Through serial-to-parallel (S/P) de-multiplexer, $L_c y_k$ is separated into $L_c y_k^s$, $L_c y_k^{1p}$ and $L_c y_k^{2p}$ corresponding to the systematic and two parity bits, respectively.

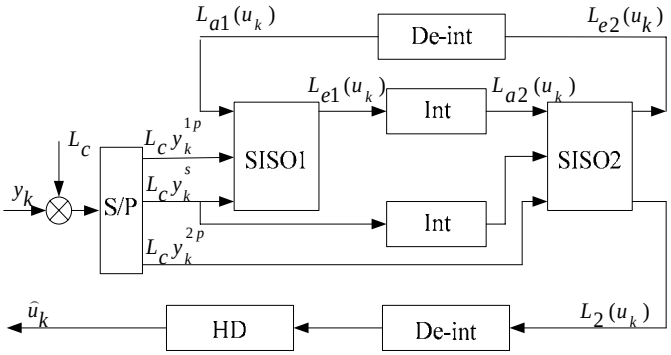

Fig. 5. ATC decoder

At the first iteration of decoding, a priori Log Likelihood Ratio (LLR) value of SISO1 decoder $L_{a1}(u_k)$ is initially set to 0, the systematic bits LLR value $L_c y_k^s$ and parity bits LLR value $L_c y_k^{1p}$ are inputted into SISO1 decoder. The extrinsic LLR value $L_{e1}(u_k)$ produced by SISO1 decoder is interleaved and sent to SISO2 decoder as a priori value $L_{a2}(u_k)$. Moreover, $L_c y_k^{2p}$ and interleaved $L_c y_k^s$ are simultaneously sent to SISO2 decoder to produce extrinsic value $L_{e2}(u_k)$, and then $L_{e2}(u_k)$ is de-interleaved (De-int) and fed back to SISO1 decoder as a priori value for the next decoding iteration. The iterative decoding will keep on working until either a stopping criteria is met or a preset maximum number of iterations is reached. When the iterative decoding is finished, the output value $L_2(u_k)$ of SISO2 decoder is de-interleaved and sent to hard decision (HD) to produce estimated value $\hat{u}_k$.

B. Proposed Two Types of ATC

Compared with STC, the constraint lengths or generator polynomials of two RSC component codes are different for ATC. Here, we design two types of ATC which consist of the parallel concatenated turbo codes using the non-identical RSC component codes with the different constraint lengths or the different types of generator polynomials.

1) Type-I of ATC:

Type-I of ATC consist of two different component codes with the identical constraint lengths but the different types of generator polynomials. As we all know, the performance of

turbo codes at low SNR is determined by the distance spectrum, but the performance at high SNR is determined by the effective free distance. There are a number of key design parameters involved in determining the distance spectrum and free distance for turbo codes, such as the choice of component encoders and the types of interleavers, etc. Several interleavers are designed to improve BER performance of turbo codes [13], [14], [15]. Here, we firstly focus all attention on using the different component codes with the primitive and non-primitive feedback generator polynomials to construct ATC, because the component codes with non-primitive generator polynomials may optimize the distance spectrum to improve water-fall performance and primitive generator polynomials may enlarge the free distance to reduce error-floor.

For convenience, the generator polynomial is denoted by G (in octal), the constraint length is denoted by K, respectively. P-G denotes primitive generator polynomial of the constituent encoder of turbo codes, NP-G denotes non-primitive polynomial. The various generator polynomials with constraint lengths K=3, 4, 5 and the types of the primitive and non-primitive polynomials are listed in Table I.

TABLE I
The various constraint lengths and the types of generator polynomials

Constraint lengths	Generator polynomials	
	P-G	NP-G
K=3	G=[7, 5]	G=[5, 5]
K=4	G=[13,17]	G=[15,17]
K=5	G=[23,35]	G=[37,21]

And then, four type-I of ATC with the same constraint lengths but mixed types of generator polynomials are presented, as shown in Table II. Here, K1 and K2 denote constraint lengths of two component codes RSC1 and RSC2, respectively ; G1 and G2 denote generator polynomials of RSC1 and RSC2, P and NP denote primitive and non-primitive polynomial, suffix 1, 2 of P and NP are corresponding to RSC1 and RSC2. We select K1=K2=5. In fact, P1-P2 and NP1-NP2 turbo codes with the same constraint lengths are just the conventional STC.

TABLE II
Type-I of ATC with the same constraint lengths and mixed types of generator polynomials

Constraint lengths	Generator polynomials			
	P1-P2	NP1-NP2	NP1-P2	P1-NP2
K1=5	G1=[23,35]	G1=[37,21]	G1=[37,21]	G1=[23,35]
K2=5	G2=[23,35]	G2=[37,21]	G2=[23,35]	G2=[37,21]

2) Type-II of ATC:

Type-II of ATC consist of two non-identical component codes with the different constraint lengths and mixed types of generator polynomials. On the one hand, the constraint length of the constituent encoder for turbo codes plays an important role in determining the performance and decoding computational complexity. Free distance is shorter for turbo codes with shorter constraint length, it can cause poorer error-floor performance. Turbo codes with longer constraint length can achieve longer free distance and better performance, but the computational complexity will increase correspondingly. In order to obtain good performance and reduce decoding computational complexity, it is necessary to decrease the constraint lengths of one constituent encoder of STC. And then, type-II of ATC can be constructed by using two component codes with different constraint lengths. On the other hand, the types of generator polynomials of component encoder are a key factor for ATC design. The primitive feedback generator polynomials for component code are known to be able to enlarge the free distance to improve error floor at high SNR, but at a cost of degrading water-fall at low SNR. On the contrary, the non-primitive generator polynomials would optimize the distance spectrum to enhance water-fall performance at low SNR, but reduce error-floor at high SNR. For this reason, type-II of ATC can also be constructed by using two component codes with mixed types of the primitive and non-primitive generator polynomials.

The constraint length K=5 of one of the constituent encoders of conventional STC in [17] is reduced to 3 and 4, primitive and non-primitive polynomial are chosen as feedback generator polynomials of two constituent codes. According to Table 1, Our proposed sixteen types-II of ATC with the different constraint lengths and mixed types of the generator polynomials are listed in Table III.

TABLE III
Types-II of ATC with different constraint lengths and mixed types of generator polynomials

Constraint lengths	Generator polynomials			
	P1-P2	NP1-NP2	NP1-P2	P1-NP2
K1=3 K2=5	G1=[7, 5] G2=[23,35]	G1=[5, 5] G2=[37,21]	G1=[5, 5] G2=[23,35]	G1=[7, 5] G2=[37,21]
K1=5 K2=3	G1=[23,35] G2=[7, 5]	G1=[37,21] G2=[5, 5]	G1=[37,21] G2=[7, 5]	G1=[23,35] G2=[5, 5]
K1=4 K2=5	G1=[13,17] G2=[23,35]	G1=[15,17] G2=[37,21]	G1=[15,17] G2=[23,35]	G1=[13,17] G2=[37,21]
K1=5 K2=4	G1=[23,35] G2=[13,17]	G1=[37,21] G2=[15,17]	G1=[37,21] G2=[13,17]	G1=[23,35] G2=[15,17]

C. Simulation and Analysis of ATC

For all simulations of two types of ATC, the information size is set to 378 bits, the constraint lengths K are 3, 4 and 5, maximum number of iteration is 8, one-half code rate, URCCC interleaver, SISO decoder, log-MAP decoding algorithm, BPSK modulation, AWGN channel.

Figure 6 gives the BER versus E_b/N_0 for the type-I of ATC with the same constraint lengths and mixed types of generator polynomials. Here, we take K1=K2=5. It was observed from the simulation results in Figure 6:

(1) The error-floor performance of P1-P2-STC is good at high SNR, but its water-fall is poor at low SNR. On the contrary, the water-fall of NP1-NP2-STC is superior at low SNR, but its error-floor is inferior at high SNR.

(2) At low SNR, the water-fall of NP1-P2-ATC and P1-NP2-ATC is superior to P1-P2-STC but inferior to NP1-NP2-STC. However, the error-floor of NP1-P2-ATC and P1-NP2-ATC is inferior to P1-P2-STC but superior to NP1-NP2-STC at high SNR.

These simulation results effectively indicate that the type-I of ATC is optimal trade-off scheme over the entire range of SNR.

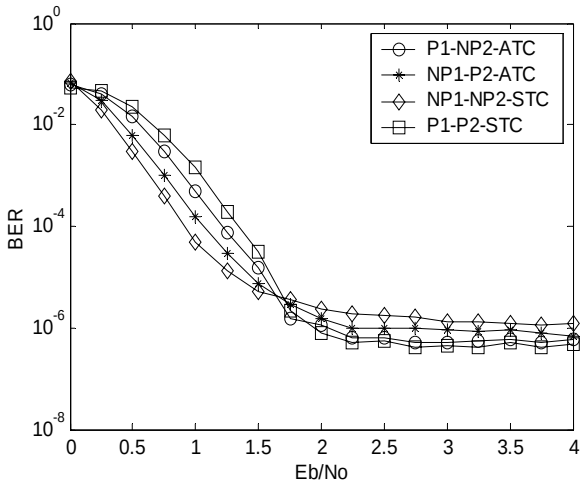

Fig. 6. BER versus E_b/N_0 for type-I of ATC with the same constraint lengths K1=K2=5 and mixed types of generator polynomials

Figure 7 shows the BER versus E_b/N_0 for the type-II of P1-P2-ATC with the different combination of the constraint lengths K=3, 4, 5 and the same primitive generator polynomials. For the ease of comparison, the BER versus E_b/N_0 for the P1-P2-STC with K1=K2=5 and primitive generator polynomials is also shown in Figure 7, the simulation analysis and conclusions are as follow:

(1) By decreasing the constraint lengths of one constituent encoder of STC, the water-fall and error-floor performances of type-II of ATC are all become deteriorated. It is caused by the smaller free distance of the component codes with short constraint lengths. However, the computational complexity of decoding algorithm can be reduced for the type-II of ATC with short constraint lengths. It is demonstrated that type-II of ATC can get a favorable trade-off between the performance and computational complexity.

(2) The performance of ATC with K1=4, K2=5 or K1=5, K2=4 is slightly inferior to STC with K1=K2=5. Especially, the performance of ATC with K1=5, K2=4 is nearly close to conventional turbo codes with negligible performance degradation but with a reduced computational complexity.

(3) The ATC with K1=5, K2=4 is superior to one with K1=4, K2=5. Similarly, the ATC with K1=5, K2=3 is superior to that with K1=3, K2=5. It is evident that reducing the constraint length of RSC2 component code is a good scheme when this type-II of ATC with the different constraint lengths are constructed.

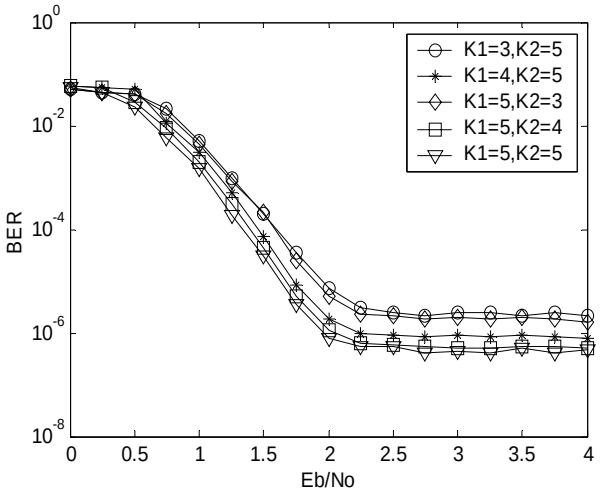

Fig. 7. BER versus E_b/N_0 for type-II of P1-P2-ATC with the different constraint lengths and the same primitive generator polynomials

The BER versus E_b/N_0 for the type-II of ATC with the different constraint lengths and mixed types of generator polynomials is shown in Figure 8. Here, we select K1=5, K2=4.

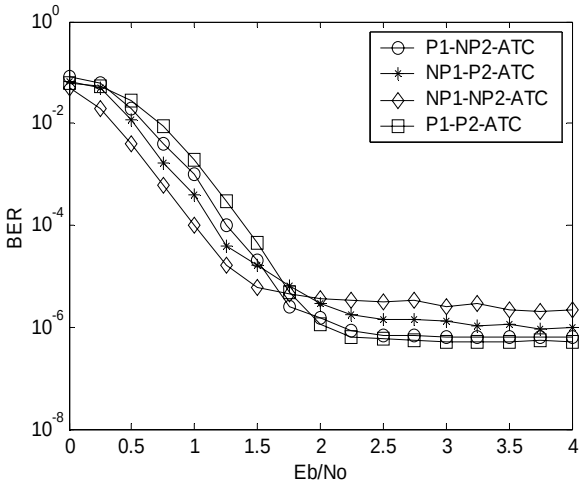

Fig. 8. BER versus E_b/N_0 for ATC with the different constraint lengths and mixed types of generator polynomials

Our analysis and conclusions from figure 8 are as follow:

(1) At low SNR ($E_b/N_0 \leq 1.75$dB), the performance of NP1-NP2-ATC is the best, NP1-P2-ATC better, P1-NP2-ATC inferior, P1-P2-ATC poor. But at high SNR ($E_b/N_0 \geq 1.75$dB), the results are in reverse order. The reason is that the non-primitive generator polynomials can optimize the distance spectrum to improve water-fall performance of turbo codes and the primitive polynomials enlarge the free distance to reduce error-floor.

(2) Considering the entire range of SNR ($0dB \leq E_b/N_0 \leq 4dB$), NP1-P2-ATC and P1-NP2-ATC are the better trade-off between the water-fall and the error-floor performance. Evidently, NP1-P2-ATC and P1-NP2-ATC are superior to P1-P2-ATC and NP1-NP2-ATC turbo codes over the entire range of SNR.

Therefore, it is a good choice that one constituent encoder is commonly constructed by using a primitive generator polynomial and another using non-primitive polynomial when this type-II of ATC are designed.

IV. JOINT SOURCE-CHANNEL CODING WITH UEP USING ATC

A. UEP Scheme using ATC

In digital multimedia communication system, the sensitivity of the image or video bit streams to channel errors is generally not uniform, the reconstructed image or video is insensitive to errors affected by insignificant bit streams (e.g. high frequency components of image), while it is rather sensitive to errors caused by significant bits (e.g. low frequency components of image), i.e. the sensitivity of the significant bits to errors is far greater than the insignificant bits. E.g. eight bits quantized gray-scale image, the priority of eight bits for per pixel is different, the sensitivity of the Most Significant Bits (MSB) to errors is greater than the Least Significant Bits (LSB). Here, we propose an UEP scheme for image transmission by using the ATC. We classify source data into several classes and use UEP encoder to strongly protect the important classes bit streams and weakly protect the non-important classes. The diagram of UEP encoder is shown in Figure 9.

According to the different importance levels, image data streams are divided into three blocks and then hierarchically coded by UEP encoder. Specific processes are as follows:

(1) Image bit streams X are partitioned into three groups so that the important bits can obtain strong protection. The first group consists of three MSB bits for per pixel, it is so called most significant bit streams X1. The second group is composed by two middle bits, named significant bit streams X2. The third group is comprised of three LSB bits, denoted as insignificant bit streams X3.

(2) In terms of different importance classes of image bit streams, the UEP encoder adaptively adopts different types of turbo codes. For X1, ATC or STC with constraint lengths K1=5 and K2=5 are chosen because they have the best performance to protect X1 strongly. For X2, ATC with constraint lengths K1=5 and K2=3 are selected due to their relative low complexity and moderate error correction ability. For X3, ATC or STC with constraint lengths K1=3 and K2=3 are chosen because of their most low complexity and lower time delay.

(3) On the conditions of CSI from channel estimator, the UEP encoder adaptively adjusts coding strategies through the switch S1, S2, S3. If the CSI is good, i.e. high SNR, then the encoder chooses P1-P2-STC or P1-P2-ATC because of their best error-floor performance. If the CSI is slightly inferior, i.e. medium SNR, then chooses NP1-P2-ATC or P1-NP2-ATC because of their best trade-off between water-fall and error-floor performance. If the CSI is worse, i.e. low SNR, then chooses NP1-NP2-STC because of their best water-fall performance.

The presented UEP scheme both considers conditions of CSI from channel estimator and the bits error effect of the different importance levels of image bit streams, it can achieve the better trade-off among the reliability, the time delay and the computational complexity.

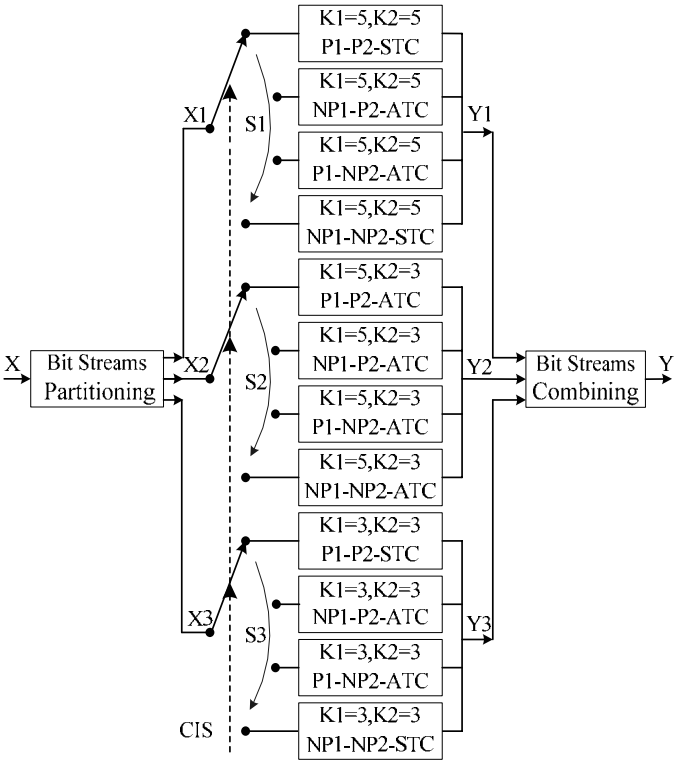

Fig. 9. UEP encoder using ATC

B. JSCC with UEP using ATC

With above mentioned UEP design using ATC, we present an effective JSCC scheme. The block diagram of the JSCC is shown in Figure 10.

Original image is firstly decomposed by discrete wavelet transformation (DWT) and compressed by SPIHT encoder [19] [20] [21]. As the importance levels of the compressed bit streams X trend towards decreasing progressively, i.e. the significant bit streams locate the nearer front and the insignificant bit streams are behind, we would partition X into three classes block, X1, X2 and X3. Then they are encoded with UEP encoder hierarchically so that the significant information can obtain strong protection. After UEP, the coded bit streams are combined to Y and modulated, then transmitted into the noisy channel. In receiver end, the received data

streams are correspondingly demodulated, UEP decoded, SPIHT decoded, inverse DWT (IDWT) and the image would be reconstructed.

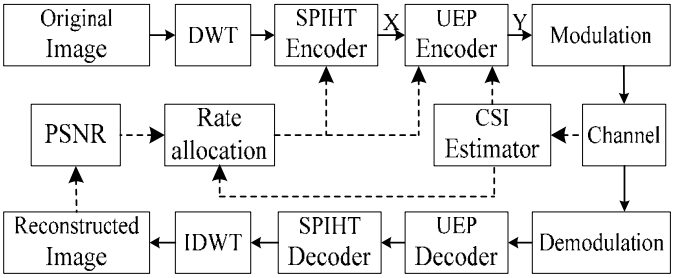

Fig. 10. Block diagram of proposed JSCC scheme based on UEP using ATC

To received data streams, the UEP decoder can be adapted to adopt various decoding algorithms and appropriate decoding iterative numbers for the different importance levels of image data streams.

(1) For received most significant data streams, UEP decoder chooses Log-MAP algorithm because of its good error correction ability. Meanwhile, properly increases decoding iterative numbers to strongly protect most significant data.

(2) For significant data, UEP decoder adopts low complicated Max-Log-MAP algorithm and moderate of the iterative numbers to reduce decoding complexity.

(3) For insignificant streams, selects lowest complexity SOVA algorithm and suitably reduces iteration numbers to further reduce computational complexity and decoding time delay.

Rate allocation in our JSCC scheme is an important part, it can optimally allocate the source CR and the channel code rates according to the calculated PSNR value of the reconstructed image and the estimated CSI condition while fixing bandwidth resource.

(1) If the calculated PSNR value is small or SNR is low, then properly increase SPIHT code rate, i.e. CR or BPP to preserve more image details. Meanwhile, select turbo coeds puncture mode to get low code rate so as to decrease the whole UEP code rate to protect image data strongly.

(2) If the PSNR is big or SNR is high, then timely reduce CR or BPP ratios to save storage size and increase UEP code rate to save channel bandwidth resource.

V. SIMULATION RESULTS AND ANALYSIS

The proposed JSCC scheme is applied to digital image communication system. Experiments are performed on 128×128 gray-scale image Lena, using 5-level wavelet decomposition based on the 9/7 tap filters, the reliability and effectiveness of the JSCC scheme was evaluated. The measure of compressed image is given by the compression ratios (CR) and the bit per pixel (BPP) ratios. CR indicates that the compressed image is stored using CR % of the initial storage size while BPP is the number of bits used to store one pixel of the image. Quality measure of the reconstructed images is given by the PSNR, where

$$PSNR = 10\log_{10}(\frac{I_{\max}^2}{MSE}) \tag{5}$$

and $I_{\max} = 255$ is the maximum pixel value for the gray-scale image when the initial pixel value is represented by 8 BPP, MSE denotes mean square error between the reconstructed image and the original image, here

$$MSE = \frac{\sum_{i=0}^{M-1}\sum_{j=0}^{N-1}[I(i,j) - I'(i,j)]^2}{MN} \tag{6}$$

M and N are the number of rows and columns of the images, I and I' are pixel value of the original image and the reconstructed image, respectively, and $0 \le i \le M-1$, $0 \le j \le N-1$.

In the transmitter, if SNR is 0-1dB, i.e. worst CSI, X1 adopts NP1-NP2-STC with K1=K2=5, X2 adopts NP1-NP2-ATC with K1=5, K2=3, X3 adopts NP1-NP2-STC with K1=K2=3. If SNR is 1-2dB, i.e. medium CSI, X1 adopts NP1-P2-ATC with K1=K2=5, X2 adopts NP1-P2-ATC with K1=5, K2=3, X3 adopts NP1-P2-ATC with K1=K2=3. And if SNR is 2-3dB, i.e. good CSI, X1 adopts P1-P2-STC with K1=K2=5, X2 adopts P1-P2-ATC with K1=5, K2=3, X3 adopts P1-P2-STC with K1=K2=3.

In the receiver, for received most significant data, the decoder chooses Log-MAP algorithm and 5 iterative. For significant data, chooses Max-Log-MAP algorithm and 4 iteration numbers. For insignificant data, selects SOVA algorithm and 3 iteration numbers. For comparison, two equal error protection (EEP) schemes using STC are also performed. In EEP, three classes bit streams all adopt NP1-NP2-STC with K=5 and 4 iteration decoding, while the decoder selects Max-Log-MAP algorithm for EEP 1 and SOVA for EEP2.

The simulation results for PSNR of JSCC with UEP and EEP in various source BPP ratios or CR and channel SNR values are listed in Table IV. The reconstructed images for JSCC with UEP and EEP in source ratio=0.5 BPP, channel SNR=1.5dB are shown in Figure 11.

From Table 4, it is obvious that the PSNR of reconstructed image for JSCC scheme with UEP using ATC is superior to EEP1 and EEP2 because the significant bit streams are strongly protected in UEP. We can see that PSNR will be better in relative higher BPP ratios with the same SNR condition, i.e. the reliability is improved, but the CR is also higher in this case, i.e. the compression effectiveness is deteriorated. We can also see that PSNR become worse in lower SNR with the same BPP ratios. To achieve the best compromise between a low CR and a good perceptual result and to adapt various channels, our JSSC scheme can optimally adjust the source BPP ratios (or CR) and channel code rates according to the calculated PSNR of the reconstructed image and the estimated SNR value.

It can be seen from Figure 11 that the reconstructed image qualities for JSCC with UEP using ATC are obviously

improved and superior to EEP1 and EEP2.

Whether objective PSNR evaluation criterion or subjective visual perceptual result, the proposed JSCC scheme is effective and feasible.

TABLE IV
PSNR (dB) of JSCC with UEP and EEP in various source ratios (BPP) and channel SNR (dB)

Source Ratio (BPP)	CR (%)	Channel SNR (dB)	PSNR (dB)		
			UEP	EEP1	EEP2
0.25	3.13	0.50	24.51	19.87	18.05
		1.50	28.84	24.65	22.32
		2.50	31.62	28.02	25.88
0.5	6.16	0.50	26.79	22.11	20.33
		1.50	31.10	27.38	25.40
		2.50	34.55	31.25	29.28
0.75	9.38	0.50	29.13	25.21	22.73
		1.50	33.22	29.80	27.69
		2.50	36.81	33.65	31.44

Fig. 11 (a)

Fig. 11 (b)

Fig. 11 (c)

Fig. 11. Reconstructed images with source ratio=0.5BPP and channel SNR=1.5dB (a) UEP (b) EEP1 (c) EEP2

VI. CONCLUSIONS

This paper presents an efficient JSCC design based on UEP using ATC, which can adaptively adopt different coding strategies, different interleavers of turbo codes, various decoding algorithms and appropriate decoding iterative numbers according to the different significant levels of image data streams and the varying conditions of estimated channel CSI. This scheme can also dynamically allocate the source ratios and channel code rates according to the calculated PSNR of reconstructed images and the estimated CSI. The proposed JSCC scheme can not only evidently improve the reconstructed image qualities but also enhance the reliability of the communication system with no additional bandwidth, our scheme is more adaptive and robust.

REFERENCES

[1] G. Cheung and A. Zakhor, "Joint source-channel coding of scalable video over noisy channels," in *IEEE Int. Conf. Image Process*., vol.3, pp. 767-770, Sep. 1996.

[2] R. Hamzaoui, V. Stankovic and Z.Xiong; "Optimized error protection of scalable image bit streams [advances in joint source-channel coding for images]," *IEEE Signal Process.*, vol. 22, no. 6, pp. 91-107, Nov. 2005.

[3] L.Yao and L. Cao, "Turbo Codes-Based Image Transmission for Channels With Multiple Types of Distortion," *IEEE Trans. Signal Process.*, vol. 17, no. 11, pp. 2112-2121, Nov. 2008.

[4] C. Lan, T. Chu, K. R. Narayanan and Z. Xiong, "Scalable image and video transmission using irregular repeat–accumulate codes with fast algorithm for optimal unequal error protection," *IEEE Trans. Commun.*, vol. 52, no. 7, pp. 1092–1101, Jul. 2004.

[5] P. G. Sherwood and K. Zeger, "Progressive image coding for noisy channels," *IEEE Signal Process. Lett*., vol. 4, no. 7, pp. 189-191, Jul. 1997.

[6] Lei Cao, "On the unequal error protection for progressive image transmission," *IEEE Trans. Image Process*., vol. 16, no. 9, pp. 2384-2388, Sept. 2007.

[7] G. Caire and G. Lechner, "Turbo codes with unequal error protection," *IET Electron.. Lett*., vol. 32, no. 7, pp. 629-631, Feb. 1996.

[8] N. Thomos, N. Boulgouris and M. Strintzis, "Wireless image transmission using Turbo codes and optimal unequal error protection," *IEEE Trans. Image Process.*, vol. 14, no. 11, pp. 1890-1901, Nov. 2005.

[9] M. Aydinlik and M. Salehi, "Turbo coded modulation for unequal error protection," *IEEE Trans. Commun.*, vol. 56, no. 4, pp. 555-564, Apr. 2008.

[10] Y.Takeshita, M.Collins and P.Massey, "A note on asymmetric Turbo codes," *IEEE Commun. Lett.*, vol. 3, no. 3, pp. 69-71, Mar. 1999.

[11] B.Shim, S.Choi, H.Park, S.Kim and Y.Ra, "A study on performance evaluation of the asymmetric Turbo codes," in *IEEE Proc. ICHIT' 08*, pp. 667-671, Aug. 2008.

[12] K.Ramasamy, B.Balakrishnan and M.Siddiqi, "A new class of asymmetric turbo code for 3G systems," *Int. J. Electron. Commun*., pp. 447-458, Jun. 2006.

[13] H.X.Wang and S.F.Liu, "A Novel Interleaver Design for Turbo Codes," *J. South-Central University for Nationalities*, vol. 29, no. 3, pp.58-60, Sep. 2010.

[14] M.Salim and S.Shrimal, "Modified interleaver design to reduce error floor in turbo codes for wireless communication," in *IEEE Proc. AMTA' 08*, pp. 698-701, Nov. 2008.

[15] S.Park and J.Jeon, "Interleaver optimization of convolutional turbo code for 802.16 systems," *IEEE Commun. Lett.*, vol. 13, no. 5, pp. 339-341, May. 2009.

[16] J.Costello, J.Hagenauer, H.Imai and B.Wicker, "Applications of error-control coding," *IEEE Trans. Inform. Theory*, vol. 44, no. 6, pp. 2531-2560, Jul. 1998.

[17] C.Berrou, A.Glavieux and P.Thitimajshima, "Near Shannon limit error-correcting coding and decoding: Turbo codes," *in IEEE Proc. ICC' 93*, pp. 1064-1070, May. 1993.

[18] J.Hagenauer, E.Offer and L.Papke, "Iterative decoding of binary block

and convolutional codes," *IEEE Trans. Inform. Theory*, vol. 42, no. 2, pp. 429-445, Mar. 1996.
[19] C.D.Creusere, "A new method of robust image compression based on the embedded zero-tree wavelet algorithm," *IEEE Trans. Image Process.*, vol. 6, no. 10, pp.1436-1442, Oct. 1997.
[20] P. Sherwood and K. Zeger, "Progressive image coding for noisy channels," *IEEE Signal Process. Lett*., vol. 4, pp. 189-191, Jul. 1997.
[21] A. Said and W. A. Pearlman, "A new fast and efficient image codec based on set partitioning in hierarchical trees," *IEEE Trans. Circuits Syst. Video Technol.*, vol. 6, no. 3, pp. 243–250, Jun. 1996.

Hanxin Wang, South-Central University for Nationalities, Wuhan, China.
Hanxin Wang received the B.S. degree in electronics and information engineering from Wuhan University, China in 1989, and finished the M.S. degree course in electronics and information engineering from South-Central University for Nationalities, China in 2002. Since 1989, he was a network engineer in Hua-zhong Computer System Engineering Company, China. During 2002-2003, as an invited visitor, he studied on wideband wireless communication in Institute of Information and Communication, Chonbuk National University, Korea. Since 2003, he was an associate professor in College of Electronics and Information Engineering, South-Central University for Nationalities, China. His research interests include information theory and modern coding theory, wideband wireless and mobile communication, cognitive radio network.

Cuitao Zhu, received the M.S. degree and the Ph.D. degree in communication and information system from Huazhong University of Science & Technology in 1999 and 2008, respectively. He is currently a professor in College of Electronics and Information Engineering, South-Central University for Nationalities, China. His research interests include wideband wireless communication, cognitive radio, compressed sensing.

Chengyi Xiong, received the M.S. degree in communication and information system in 2000 from South-Central University for Nationalities, and the Ph.D. degree from Huazhong University of Science & Technology in 2006. He is currently a professor in College of Electronics and Information Engineering, South-Central University for Nationalities, China. His research interests include signal processing, compressed coding of image and video, compressed sensing.

Shaoping Chen, received the M.S. degree in communication and information system in 1990 from Wuhan University, and the Ph.D. degree from Huazhong University of Science & Technology in 2004. He is currently a professor in College of Electronics and Information Engineering, South-Central University for Nationalities, China. His research interests include high speed wireless communication, digital signal processing, MIMO system, OFDM technique.